

REPORT DOCUMENTATION PAGE

Form Approved
OMB No. 0704-0188

Public reporting burden for this collection of information is estimated to average 1 hour per response, including the time for reviewing instructions, searching existing data sources, gathering and maintaining the data needed, and completing and reviewing this collection of information. Send comments regarding this burden estimate or any other aspect of this collection of information, including suggestions for reducing this burden to Department of Defense, Washington Headquarters Services, Directorate for Information Operations and Reports (0704-0188), 1215 Jefferson Davis Highway, Suite 1204, Arlington, VA 22202-4302. Respondents should be aware that notwithstanding any other provision of law, no person shall be subject to any penalty for failing to comply with a collection of information if it does not display a currently valid OMB control number. **PLEASE DO NOT RETURN YOUR FORM TO THE ABOVE ADDRESS.**

1. REPORT DATE (DD-MM-YYYY)		2. REPORT TYPE Technical Papers		3. DATES COVERED (From - To)	
4. TITLE AND SUBTITLE				5a. CONTRACT NUMBER	
				5b. GRANT NUMBER	
				5c. PROGRAM ELEMENT NUMBER	
6. AUTHOR(S)				5d. PROJECT NUMBER 1011	
				5e. TASK NUMBER CA9F	
				5f. WORK UNIT NUMBER	
7. PERFORMING ORGANIZATION NAME(S) AND ADDRESS(ES) Air Force Research Laboratory (AFMC) AFRL/PRS 5 Pollux Drive Edwards AFB CA 93524-7048				8. PERFORMING ORGANIZATION REPORT	
9. SPONSORING / MONITORING AGENCY NAME(S) AND ADDRESS(ES) Air Force Research Laboratory (AFMC) AFRL/PRS 5 Pollux Drive Edwards AFB CA 93524-7048				10. SPONSOR/MONITOR'S ACRONYM(S)	
				11. SPONSOR/MONITOR'S NUMBER(S)	
12. DISTRIBUTION / AVAILABILITY STATEMENT Approved for public release; distribution unlimited.					
13. SUPPLEMENTARY NOTES					
14. ABSTRACT <div>20030110 130</div>					
15. SUBJECT TERMS					
16. SECURITY CLASSIFICATION OF:			17. LIMITATION OF ABSTRACT A	18. NUMBER OF PAGES	19a. NAME OF RESPONSIBLE PERSON Leilani Richardson
a. REPORT Unclassified	b. ABSTRACT Unclassified	c. THIS PAGE Unclassified			19b. TELEPHONE NUMBER (include area code) (661) 275-5015

Standard Form 298 (Rev. 8-98)
Prescribed by ANSI Std. Z39.18

18 separate items enclosed

1011CA9F TP-FY99-0072

✓ Spreadsheet
✓ DTS

MEMORANDUM FOR PRS (Contractor Publication)

FROM: PROI (TI) (STINFO)

4 May 1999

SUBJECT: Authorization for Release of Technical Information, Control Number: **AFRL-PR-ED-TP-FY99-0072**
Dan Baron (ERC), "Fracture Parameter Calculations for SENT Specimens with Two Boundary
Conditions"

SEM

(Statement A)

Fracture Parameter Calculations for SENT Specimens with Two Boundary Conditions

D.T. Baron
ERC Inc.
AFRL
Room 111
Building 8424
3 Antares Road
Edwards AFB, CA 93524

INTRODUCTION

This paper is about finite element calculations of the Mode I stress intensity factor (K_I), and the T-stress (T), for single edge-notched tension (SENT) specimens. Linear elastic fracture mechanics (LEFM) is used. (4) cases of traction application method and plane state (TAMPS) are considered, applied uniform load and plane stress (LS), applied uniform load and plane strain (LN), applied uniform displacement and plane stress (DS), applied uniform displacement and plane strain (DN). For all cases, the material is considered to be incompressible, i.e., 0.5 is used for Poisson's ratio (ν). Young's modulus is referred to as E . The total height (perpendicular to the crack) of a SENT specimen is called h , and the total width (parallel to the crack) is called w . The crack length is called a .

FINITE ELEMENT CALCULATIONS

The ABAQUS finite element program, version 5.6 was used. All calculations were for a linear material with small strains and small displacements. Figure 0 shows the general form of the finite element meshes. One half of each SENT specimen was modeled, cut through the line of symmetry, the crack line. In Figure 0, the 'y's along part of the bottom of the mesh, indicate that each point ahead of the crack tip along a mesh's bottom edge was constrained from displacement in the y direction. The 'x's along the top of the mesh indicate that each point along a mesh's top edge was constrained from displacement in the x direction. (The top edge x constraint was used to simulate the gluing of an experimental specimen to an end fixture.) Each mesh was divided into 16 element sectors of approximately equal angle radiating from the crack tip. Each mesh was divided into 64 element orbits about the crack tip. Each mesh consisted of $16 \times 64 = 1024$ elements. The elements were rectangular 8 node (one node at each corner, one node on each side) isoparametric. Each crack tip element was formed by positioning the (3) nodes along one side at the crack tip. All of the crack tip nodes were tied together. Element corner nodes were located at the intersection of the sector lines and orbit curves. Element side nodes were located midway between the corner nodes. The nodes on the radial sides of the crack tip elements were located at the quarter points.

The family of orbit curves was constructed so that the innermost curve was circular. The shapes of the curves gradually became more rectangular nearer to the mesh boundaries (the two sides and the top). Beginning at the crack tip, the distances between adjacent orbit curves increased linearly in the $-x$, $+x$, and $+y$ directions. The radius of the innermost (circular) orbit curve was $w/10^4$. (396) (4 TAMPS * $11 h/w$ * $9 a/w$) ABAQUS problems were solved to generate the included data. A FORTRAN 90 program was written and used to automatically generate a mesh and ABAQUS input file from the values of a number of variables in a parameter file. ABAQUS was run on a UNIX machine. Typically, 99 runs were made at one time from a batch file running overnight.

THEORY AND NUMERICAL IMPLEMENTATION

Figures 1-4 show the T-stress parameter β plotted versus the crack ratio. β is defined as

$$\beta \equiv \frac{T\sqrt{\pi a}}{K_I} \quad (1)$$

K_I is equal to

$$K_I = \sqrt{J E'} \quad (2)$$

J is the energy release rate at the crack tip. E' is defined as

$$E' \equiv \begin{cases} E & \text{(plane stress)} \\ \frac{E}{1-\nu^2} & \text{(plane strain)} \end{cases} \quad (3)$$

ABAQUS has a command to calculate J , and uses the energy domain integral method. For each ABAQUS run, 64 calculations of J were made, one for each element orbit curve. For each run, all 64 J values were close to identical.

Williams [1] showed that the stresses in a linear elastic body can be written in an infinite series expansion. Near the crack tip the effect of the higher order terms can be neglected, and σ_{xx} can be written as

$$\sigma_{xx} = \frac{K_1}{\sqrt{2\pi}} \cos\left(\frac{\theta}{2}\right) \left[1 - \sin\left(\frac{\theta}{2}\right) \sin\left(\frac{3\theta}{2}\right) \right] + T. \quad (4)$$

Along the crack flank ($\theta = \pi$), the first term in Equation (4) is zero, and σ_{xx} becomes

$$\sigma_{xx} = T. \quad (5)$$

Therefore, along the crack flank, and near the crack tip, a finite element calculation of σ_{xx} should be approximately equal to T . Ayatollahi [2] has shown that a better approximation for T can be determined by using

$$\sigma_{xx} = T = E' \frac{du_x}{dx}, \quad (6)$$

where u_x is the displacement along the crack flank in the x direction. For the data of this paper, T was calculated using Equation (6). du_x/dx was approximated by fitting a least squares line to the data points (x, u_x) of the nodes on the crack flank within the distance of $a/10$ of the crack tip.

Figures 5-8 show normalized T-stress (T/σ_∞) plotted versus the crack ratio. σ_∞ is the specimen's average end stress; i.e., the sum of the mesh top edge nodal forces in the y direction divided by w . (For cases LS and LN these nodal forces were applied, and for cases DS and DN they were induced.)

NUMERICAL RESULTS

Each of Figures 1-8 shows 11 curves, one for each of the specimen aspect ratios $h/w = \{1/4, 1/3, 1/2, 1/1, 2/1, 3/1, 4/1, 5/1, 6/1, 7/1, 8/1\}$. Each curve was constructed using 9 points, for the crack ratios $a/w = \{0.05, 0.10, 0.20, 0.30, 0.40, 0.50, 0.60, 0.70, 0.80\}$.

Notice that for a SENT experimental specimen, both T and K_1 can be determined using the figures. Since σ_∞ is either applied or measured, one of Figures 5-8 will give T . Once T is known, the corresponding figure of Figures 1-4 will give K_1 .

Figures 1 and 5 were compared to Figure 4 from the T-stress compendium by Sherry [3], and showed reasonable agreement.

The figures generally show that the fundamental characters of the curves change when the specimen aspect ratio (h/w) is less than 1. There is little difference between the effects of plane stress and plane strain when uniform load is prescribed (cases LS and LN). However when uniform displacement is prescribed (cases DS and DN) the differences between plane stress and plane strain can be significant, especially for $h/w < 1$. The figures show that both β and T/σ_∞ crucially depend on whether uniform load or uniform displacement is applied to a specimen. One condition should never be used to approximate the other.

CONCLUSIONS

The boundary condition of Figure 0 (in which the entire mesh top edge was constrained in the x direction) was used because it seems to be the only condition that can be practically implemented. Devising an experimental method to constrain only one point in the x direction seems difficult. The result is that for values of $h/w < 1$, relatively huge T-stresses can be generated.

Applying a load to a SENT specimen that is even approximately uniform seems to be an impossibility, unless the specimen is extremely long. Even if the end fixtures are pinned at their middles, the most that can be said is that the centroid of the end loads are located at the pin centers.

For experimental single edge-notched tension specimens, calculations using uniform applied load should never be substituted for calculations using uniform applied displacement when determining values of the stress intensity factor (K_1) and the T-stress (T).

REFERENCES

1. Williams, M.L.: "On the Stress Distribution at the Base of a Stationary Crack." *Journal of Applied Mechanics*: Volume 24: 109-114: 1957.
2. Ayatollahi, M.R.; Smith, D.J.; Pavier, M.J.: *Displacement Based Approach To Obtain T-Stress Using Finite Element Analysis*: PVP-Vol. 346, Fatigue and Fracture: Volume 2: 149-154: 1997.
3. Sherry, A.H.; France, C.C.; Goldthorpe, M.R.: *Compendium Of T-Stress Solutions For Two And Three Dimensional Cracked Geometries: Fatigue & Fracture of Engineering & Structures*: Volume 18: No. 1: 141-155: 1995.

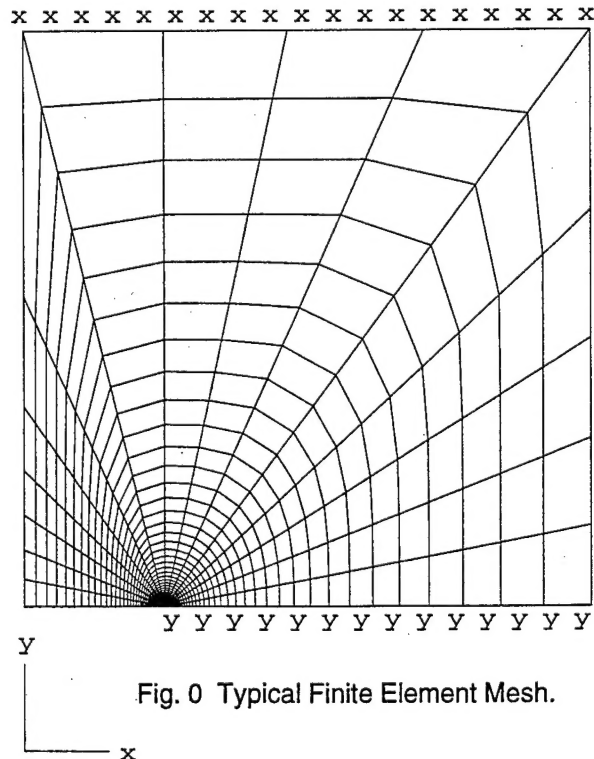


Fig. 0 Typical Finite Element Mesh.

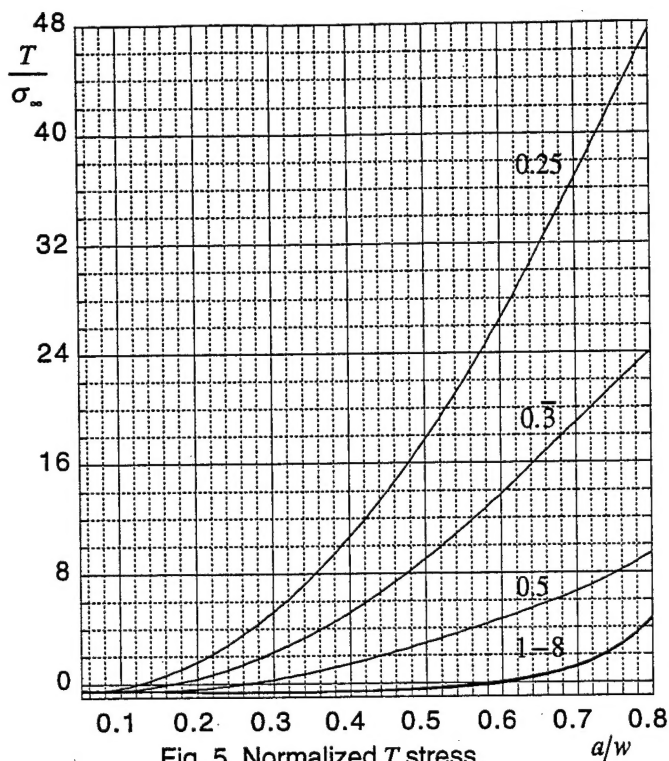


Fig. 5 Normalized T stress.
Applied uniform load.
Plane stress.

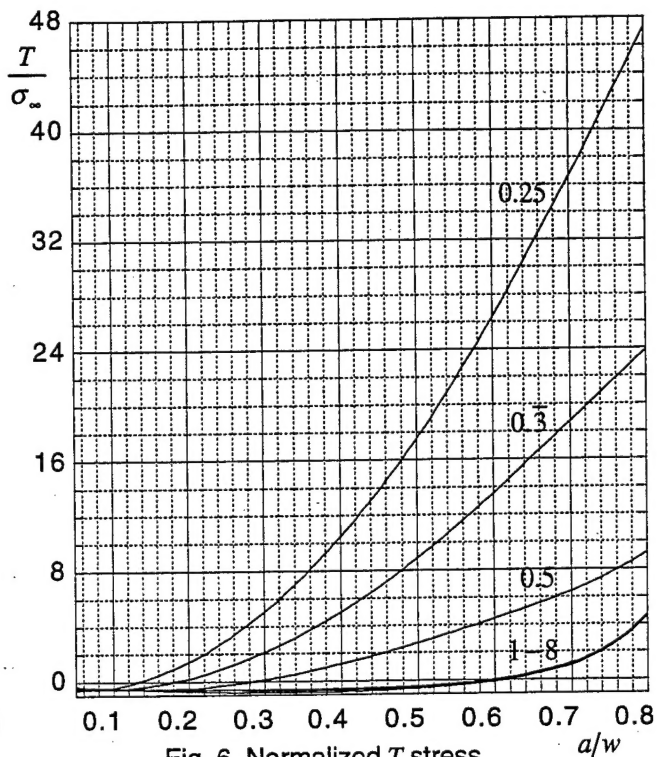


Fig. 6 Normalized T stress.
Applied uniform load.
Plane strain.

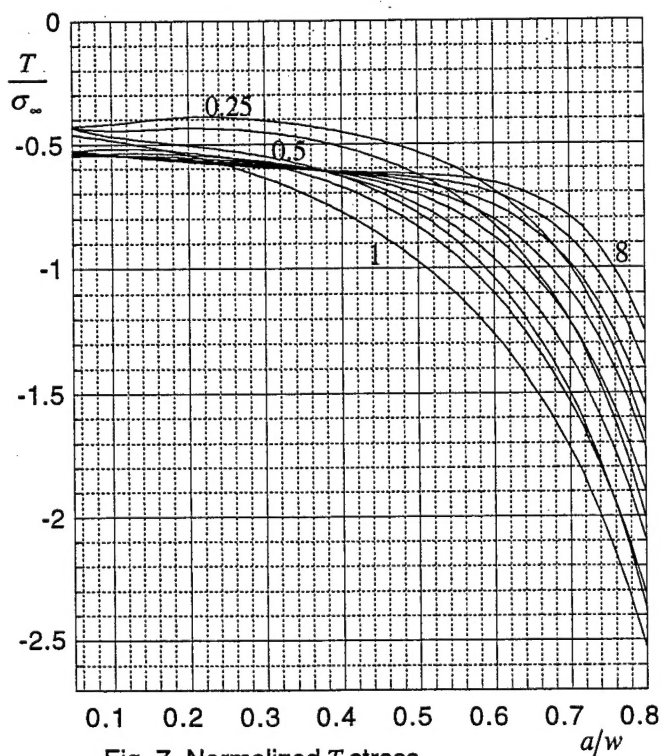


Fig. 7 Normalized T stress.
Applied uniform displacement.
Plane stress.

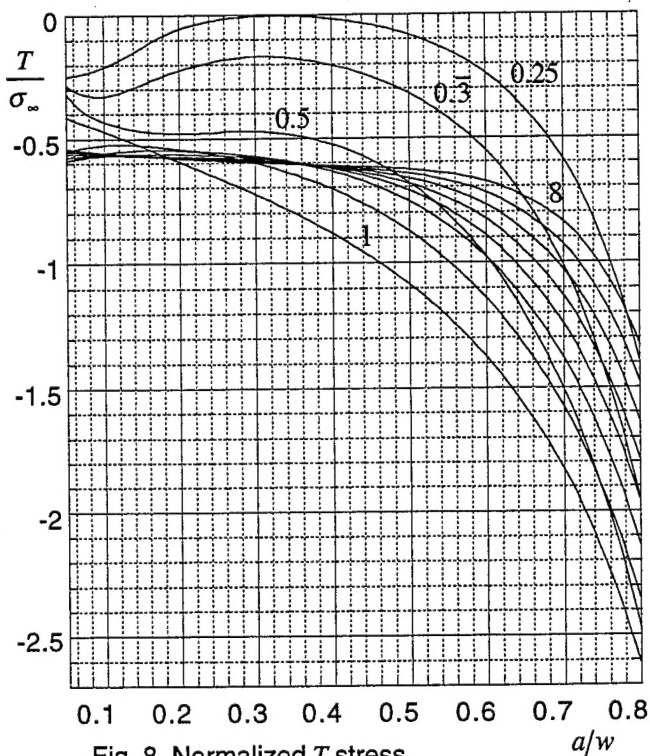


Fig. 8 Normalized T stress.
Applied uniform displacement.
Plane strain.

PAGES fig 1, 2, 3, 4
ARE
MISSING
IN
ORIGINAL
DOCUMENT